

# Orbit response matrix measurements for 10Hz global orbit feedback in RHIC

C. Liu,

October 2010

Collider Accelerator Department  
**Brookhaven National Laboratory**

**U.S. Department of Energy**

USDOE Office of Science (SC)

Notice: This technical note has been authored by employees of Brookhaven Science Associates, LLC under Contract No. DE-AC02-98CH10886 with the U.S. Department of Energy. The publisher by accepting the technical note for publication acknowledges that the United States Government retains a non-exclusive, paid-up, irrevocable, world-wide license to publish or reproduce the published form of this technical note, or allow others to do so, for United States Government purposes.

## **DISCLAIMER**

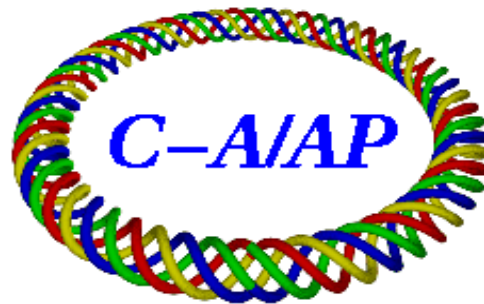
This report was prepared as an account of work sponsored by an agency of the United States Government. Neither the United States Government nor any agency thereof, nor any of their employees, nor any of their contractors, subcontractors, or their employees, makes any warranty, express or implied, or assumes any legal liability or responsibility for the accuracy, completeness, or any third party's use or the results of such use of any information, apparatus, product, or process disclosed, or represents that its use would not infringe privately owned rights. Reference herein to any specific commercial product, process, or service by trade name, trademark, manufacturer, or otherwise, does not necessarily constitute or imply its endorsement, recommendation, or favoring by the United States Government or any agency thereof or its contractors or subcontractors. The views and opinions of authors expressed herein do not necessarily state or reflect those of the United States Government or any agency thereof.

C-A/AP/#407

Oct. 2010

# Orbit Response Matrix Measurements for 10Hz Global Orbit Feedback in RHIC

C. Liu, M. Minty



**Collider-Accelerator Department  
Brookhaven National Laboratory  
Upton, NY 11973**

Notice: This document has been authorized by employees of Brookhaven Science Associates, LLC under Contract No. DE-AC02-98CH10886 with the U.S. Department of Energy. The United States Government retains a non-exclusive, paid-up, irrevocable, world-wide license to publish or reproduce the published form of this document, or allow others to do so, for United States Government purposes.

# Orbit response matrix measurements for 10Hz global orbit feedback in RHIC

C. Liu, M. Minty

## 1. Introduction

The 10 Hz global orbit feedback system (gofb) was designed to correct the 10 Hz horizontal beam perturbations in both rings that are suspected to be caused by vibrations of the final focusing quadrupoles (triplets) [1, 2]. The full system envisioned for Run-11 consists of 36 BPMs, corresponding to 2 per triplet in each of the 12 triplet locations and two in each of the 6 arcs, and 1 dipole corrector at each triplet location for a total of 12 correctors. Prototype testing was successfully carried out during RHIC Run-10 in store condition with 4 new dipole correctors (with independent power supplies) and 8 stripline beam position monitors (BPMs) per accelerator. An SVD-based algorithm was used to compute the applied corrections. For Run-10, the response matrix was provided by W. W. MacKay. The response matrix  $R$  relates corrector angles to beam displacements at BPMs.

$$\Delta x = R\Delta\theta \quad (1)$$

For Run-10, the matrix  $R$  was 8 by 4 in dimensions

$$\begin{pmatrix} \Delta x_1 \\ \Delta x_2 \\ \dots \\ \Delta x_8 \end{pmatrix} = \begin{pmatrix} R_{11} & R_{12} & R_{13} & R_{14} \\ R_{21} & R_{22} & R_{23} & R_{24} \\ \dots & \dots & \dots & \dots \\ R_{81} & R_{82} & R_{83} & R_{84} \end{pmatrix} \begin{pmatrix} \Delta\theta_1 \\ \Delta\theta_2 \\ \Delta\theta_3 \\ \Delta\theta_4 \end{pmatrix}, \quad (2)$$

where  $R_{ij}$  is the closed-loop transfer function which correlates corrector strength  $\Delta\theta_j$  and horizontal position measured by a beam position monitor  $\Delta x_i$ .

Eq. (2) was used to calculate the response matrix  $R$ , and furthermore to solve for the required corrector strength based on the beam position measurements using SVD or least-square algorithm [3] with the  $R$  as derived from the online optical model (OptiCalc). In order to generate a more accurate (direct measurement avoids errors in BPM and corrector calibrations and in the optical model) response matrix  $R$ , ORM measurements were performed in both accelerators during Run-10. The correctors were driven sequentially at 12 Hz; the BPM values were recorded at a sampling rate of 1 kHz. In this report, we mainly discuss how to generate the response matrix for each ring using experimental data acquired during system prototyping in Run-10.

## 2. Data

For the list of correctors and BPMs used in Run-10, please check this link:

[http://www.cadops.bnl.gov/Instrumentation/InstWiki/index.php/Orbit\\_Feedback,\\_10\\_Hz\\_Global#Run-10](http://www.cadops.bnl.gov/Instrumentation/InstWiki/index.php/Orbit_Feedback,_10_Hz_Global#Run-10)

The data were taken on Apr. 15<sup>th</sup>, 2010, for fill 12183 at 39 GeV Au-Au run. As an example, the beam positions from BPM bo6-b1 (first BPM counting from 6 o'clock clockwise) is shown in Fig.1 as each of the 4 correctors were excited consecutively from the blue ring.

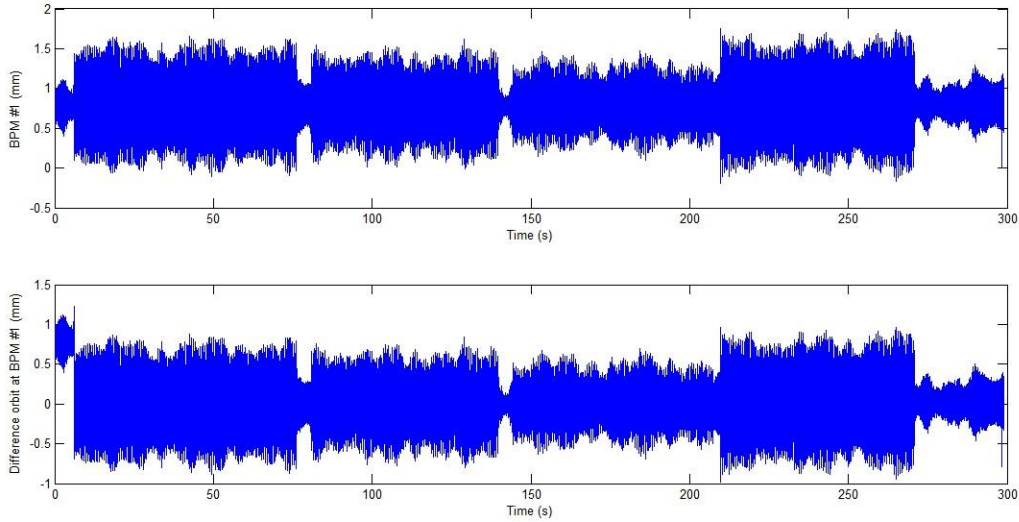


Fig. 1 Beam positions from BPM #1

The upper plot shows the raw data after removal of spurious zero readings. The average beam position was calculated for the first several seconds with all correctors off. By subtracting the average, the relative beam displacements due to the corrector excitations are shown in the lower plot. The corresponding corrector angles are shown in Fig. 2, showing the envelope of the applied 12 Hz excitations, where the conversion to angles was made using angle to current ratio as  $6.103 \times 10^{-7}$  mrad/ADC count of current readback [4] at 39 GeV for Au beam. The red squares indicate the start and end points. Here, too, the zeroes from LogView have been eliminated. The peak-to-peak amplitude was  $1 \times 10^{-2}$  mrad.

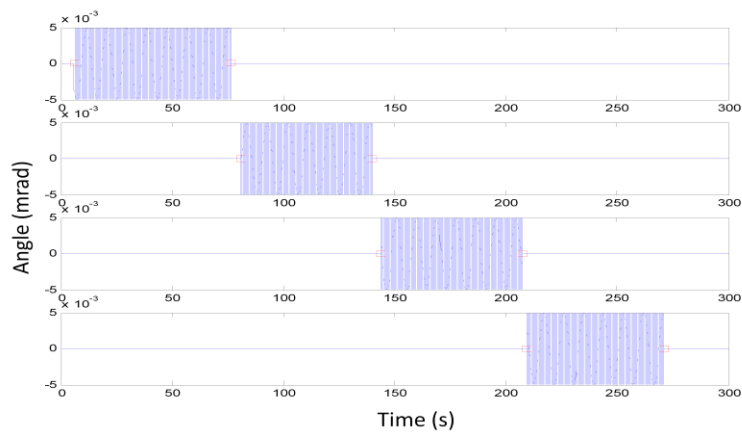


Fig. 2 The strength of correctors: from top to bottom, correctors are at 6, 7, 8 and 5 o'clock

### 3. Data analysis

We evaluated three different methods for generating the response matrix from the experimental data. All methods aim to extract the slope  $\Delta x/\Delta\theta$  due to the applied excitation while minimizing contributions due to other sources of perturbation to the beam trajectory such as from the triplet vibrations. One of the methods for calculating the response matrix R is to create correlation plots between the 8 BPMs and 4 correctors (Fig. 3), perform linear fitting, extract 32 slopes  $\Delta x/\Delta\theta$  corresponding to the 32 elements of matrix R. The other two equivalent methods require determination of the amplitudes of beam displacement at the applied excitation frequency. The ratio of this amplitude to corrector strength amplitude gives the matrix elements (Fig. 4). Extracting the beam response was evaluated in both the time and frequency domains using curve fitting and fast Fourier transforms (FFT) respectively. In the following, data analysis (mostly for blue ring) will be presented.

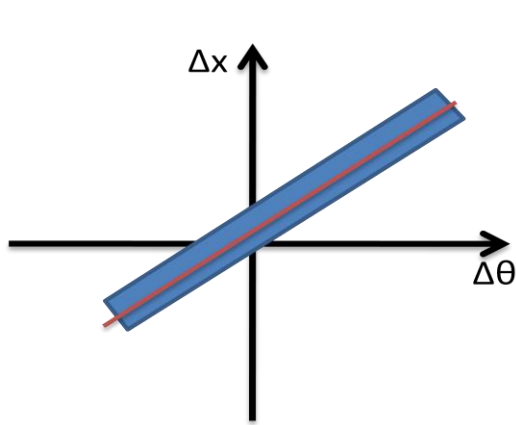


Fig. 3 Correlation plot and linear fitting

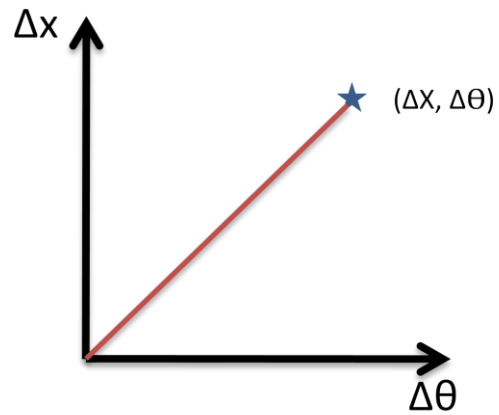


Fig. 4 Ratio of two amplitudes

#### (1). Linear fitting

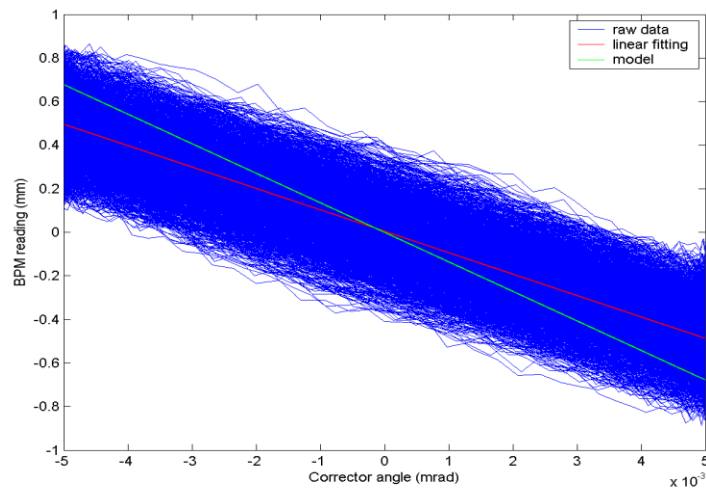


Fig. 5 Linear fitting for BPM #1 and corrector #1 correlation plot

Fig. 5 shows linear fitting result for BPM #1 and corrector #1 correlation plot. The blue curves are from the raw data. A fairly wide band is observed due to beam oscillations at other frequencies (dominated by multiple excitation sources near 10 Hz) other than 12 Hz. The red line is from the linear least square fit while the green line (model) is from the matrix element provided by W. W. MacKay.

The fitted and model slopes for all 32 transfer function elements are given in Fig. 6, which is arranged to correspond to the elements of  $R^T$ .

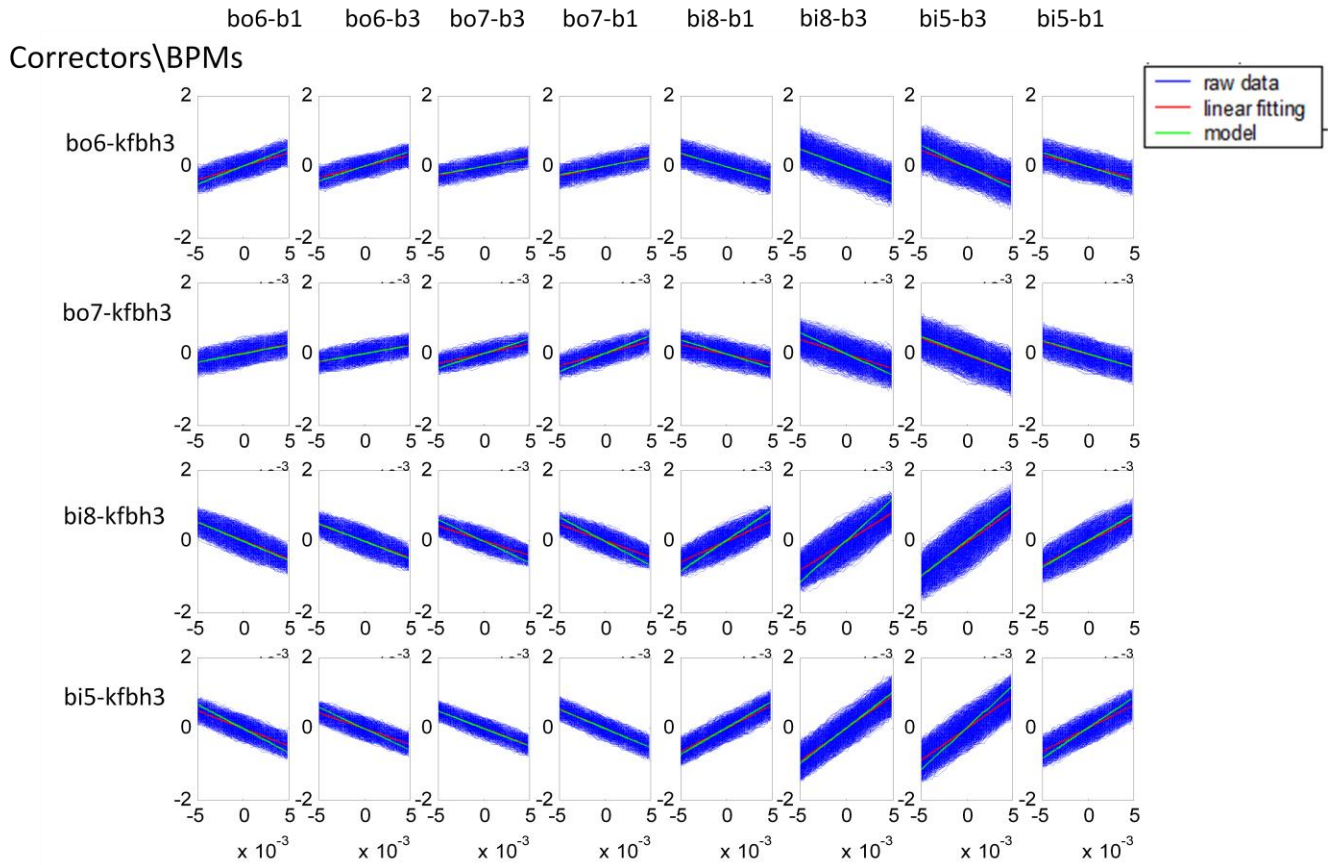


Fig. 6 Measured beam positions (mm) as a function of corrector angles (mrad) (blue band); linear fitting (red line) compared to model slope (green line) for blue ring

The results for the yellow ring are shown in Fig. 7. For comparison, the numerical values generated from the measured data and those from the RHIC model matrix for blue ring are listed in Appendix A.

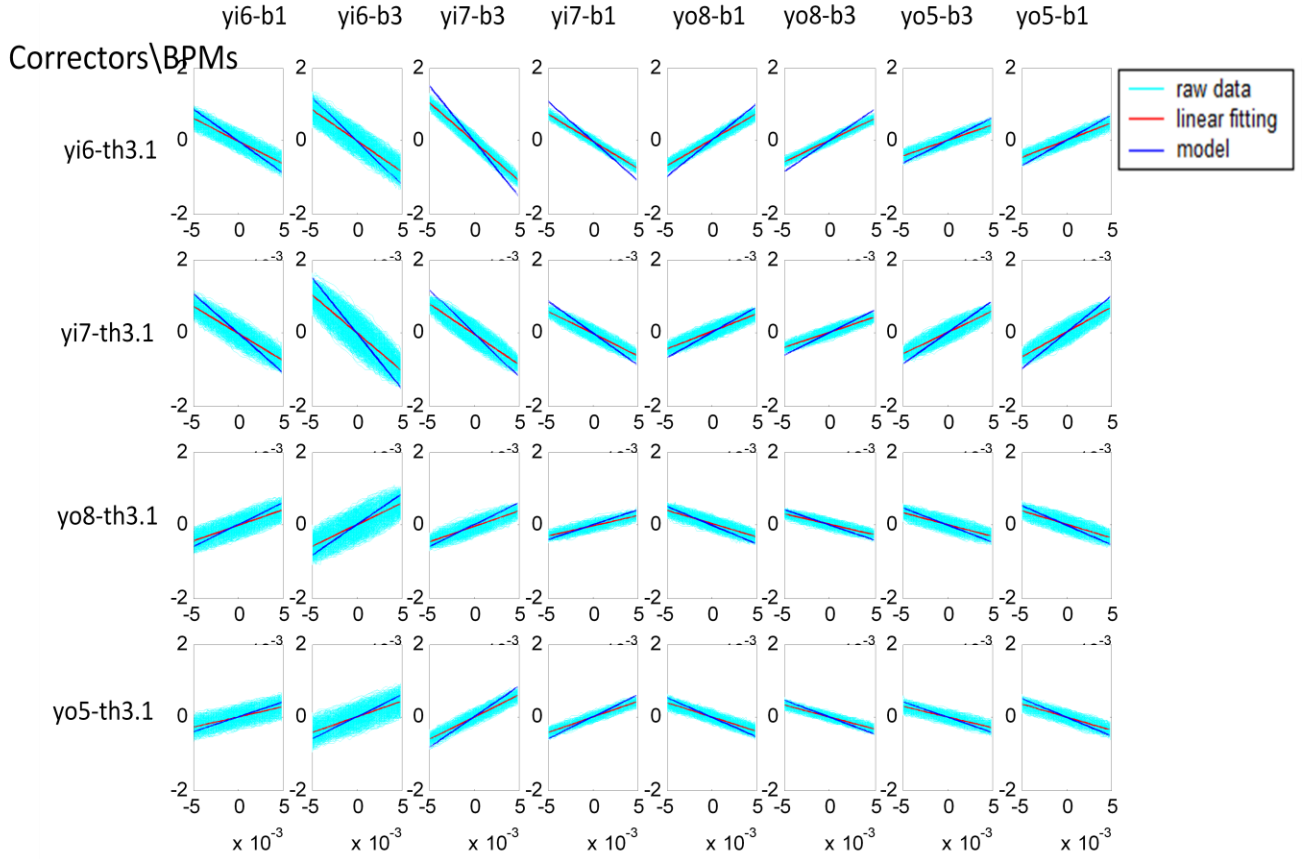


Fig. 7 Measured beam positions (mm) as a function of corrector angles (mrad) (cyan band); linear fitting (red line) compared to model slope (blue line) for yellow ring

In the next two sections, we fit for the beam amplitude response using the other two methods mentioned before.

## (2). Finding amplitude by curve fitting

Because of the presence of the other frequencies (dominated by the 10 Hz), beating of two dominating frequencies (10 Hz and 12 Hz) is clearly observed in the BPM measurements as shown in Fig. 8. To determine the amplitude of the beam response to the applied 12 Hz oscillation, curve fitting of the BPM measurements is used. The equation for curve fitting is

$$x(t) = A_1 \cos(2\pi \cdot f_1 \cdot t + \varphi_1) + A_2 \cos(2\pi \cdot f_2 \cdot t + \varphi_2), \quad (3)$$

where  $A_1$ ,  $A_2$  are the amplitudes, and  $\varphi_1$ ,  $\varphi_2$  are the phases of the components at dominant frequencies  $f_1$  and  $f_2$ . These two frequencies were obtained by Fourier analysis of the BPM measurements yielding as the two most dominant sources of excitation  $f_1 = 12.06$  Hz and  $f_2 = 10.16$  Hz.



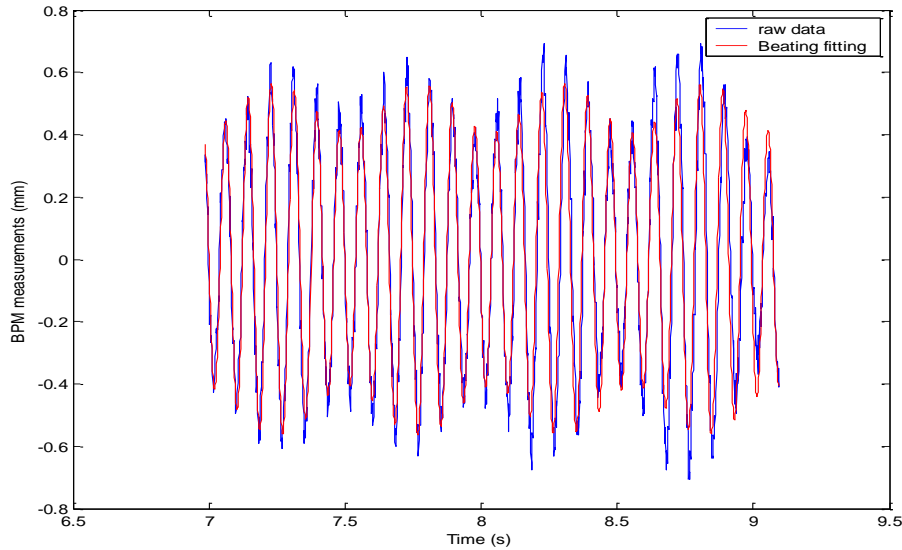


Fig. 8 BPM measurements evidencing strong modulation (beating) and least square fit using two dominant frequencies

Shown in Fig. 8 are the raw data and fitted curve for BPM bo-b1 (#1) while exciting corrector bo6-kfbh3 (#1). The fitting results are:  $A_1=0.486$  mm,  $\phi_1=-66.1^\circ$ ,  $A_2=0.078$  mm,  $\phi_2=-329.8^\circ$ . Neglecting the sign of the coefficient, the transfer function correlates corrector #1 and BPM #1, which is the 1<sup>st</sup> element of the response matrix,  $R_{11}=A_1/\Delta\theta=97.1$  mm/mrad. Repeating this for all BPM and corrector combinations, the response matrix generated is shown in Appendix A.

The deviation in absolute value of the elements of the two matrices ( $R_{curvefit}$  and  $R_{linefit}$ ) is about 2%, which verifies the linear fitting result. The sign of the elements of  $R_{curvefit}$  is obtainable by inspection of the relative phase of BPMs and correctors: the sign is positive if in phase or negative if out-of-phase. This can be done manually or numerically as shown in section 3.

### (3). Amplitude from fast Fourier transforms (FFT)

In MatLab, the resulting FFT amplitude is

$$A(w) = A*n/2, \quad (4)$$

where A is the time domain amplitude and n is the number of data points. This is true only if the number of FFT points is greater than or equal to the number of data samples. If the number of FFT points is less, the FFT amplitude is lower than the original amplitude by the above amount ( $A*n/2$ ). Therefore, the amplitude of a particular frequency (12 Hz in this case) can be derived according to Eq. (4) with zero padding of the original signal (to approximately 4 times the original length) before performing the Fourier transform. Figure 9 shows the FFT of BPM #1 measurement obtained with excitation of corrector #1. The corresponding matrix element is calculated to be 96.4 mm/mrad.

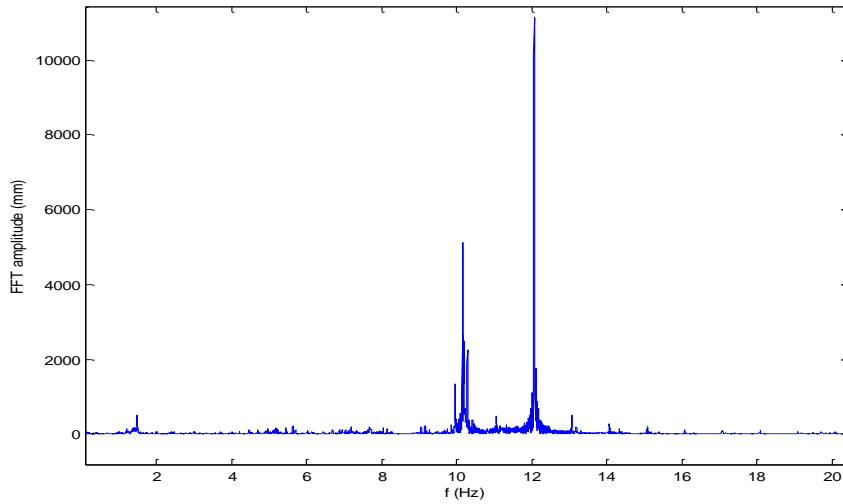


Fig. 9 FFT of BPM #1 readings

By doing so for all BPMs and correctors, the matrix  $R_{\text{fft}}$  is generated as shown in Appendix A.

The deviation in absolute values for three matrices,  $R_{\text{linearfit}}$ ,  $R_{\text{curvefit}}$  and  $R_{\text{fft}}$ , is about 8%. The numerical results obtained using the three methods described in the last sections given in Appendix A are shown in Fig.10.

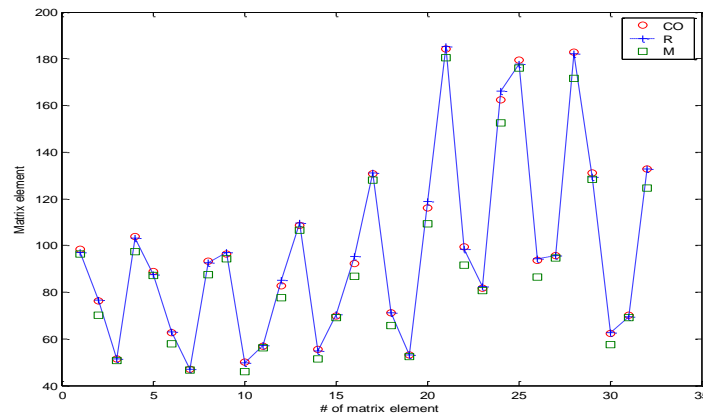


Fig. 10 Comparison of the elements of the three matrices obtained from linear fitting (red circles), curve fitting (blue plus) and FFT (green square)

As mentioned earlier, the last two methods used to extract the beam response at the applied frequency gave absolute value only. The sign of each matrix element can be derived by inspection of the relative phases between BPMs and correctors by comparing the phases at BPMs and correctors at the applied excitation frequency derived from the FFT. This results in a matrix of relative phases for blue ring

$$D_{\text{phi}} = \begin{bmatrix} -3.7186 & -3.7294 & -3.6935 & -3.6278 & 176.2954 & 176.3304 & 176.3897 & 176.3945 \end{bmatrix}$$

-11.1535	-11.1525	-11.1676	-11.1579	168.8382	168.8489	168.9091	168.9264
166.9861	166.9564	166.9611	166.9846	-13.0145	-13.0054	-12.9245	-12.9204
176.1949	176.1882	176.2763	176.2554	-3.6929	-3.6920	-3.7189	-3.7153

in units of degrees. As an example, the beam responses to a pure applied sine excitation only. Then, the response detected at a BPM is either in phase (0 degree relative phase) or out of phase (180 degree) with respect to the correctors since the transit time between corrector and BPM is negligible. However, small deviation from 0 and 180 degree relative phase are presented because of 10 Hz distortion. A sign matrix was generated with elements set to +1 if the relative phase in Dphi above was close to 0 degree and set to -1 if relative phases close to 180 degree.

sgn =

1	1	1	1	-1	-1	-1	-1
1	1	1	1	-1	-1	-1	-1
-1	-1	-1	-1	1	1	1	1
-1	-1	-1	-1	1	1	1	1

This sign matrix agrees with the signs from linear fitting in section 1.

#### 4. Orbit response matrix (ORM) calculation

The three methods described above are in relatively good agreement, however markedly different from the model used both in the analysis and as used in the feedback algorithm. We next checked this model matrix using Twiss parameters derived from the online OptiCalc model.

Based on [5], the closed orbit at an arbitrary position  $s$  with a corrector (kick angle  $\theta$ ) at position  $s_0$  is

$$y_{co}(s) = G(s, s_0)\theta(s_0),$$

where

$$G(s, s_0) = \frac{\sqrt{\beta(s)\beta(s_0)}}{2 \sin \pi \nu} \cos(\pi \nu - |\psi(s) - \psi(s_0)|)$$

is the Green function of Hill's equation. The orbit response arising from a dipole kick is given by the product of the Green function and the kick angle. A slightly different formula is presented in [6].

In [7], calculation of the ORM from transfer matrix is elaborated. Using the Twiss parameters<sup>1</sup> extracted from OptiCalc, ORM are calculated based on the models in [5-7]. Not surprisingly, the three matrices<sup>2</sup> are exactly the same. It is shown below (in units of mm/mrad)

OR=97.114665	79.637262	44.525924	47.496605	-71.972745	-95.522690	-115.018861	-76.577796
46.008402	43.365714	80.358129	98.011852	-77.20140	-115.936201	-94.134591	-71.176113
-104.094018	-95.584095	-122.259520	-136.568111	171.253952	234.032360	195.181499	145.369037
-131.637426	-118.111446	-96.008545	-104.891845	144.569350	194.589352	227.386799	166.721600

<sup>1</sup> see appendix A for Twiss parameters at correctors and BPMs in blue ring

<sup>2</sup> see appendix B for the MatLab code for calculating the ORM

The matrix elements are plotted in Fig. 11 together with the model matrix provided by W. W. MacKay, which shows excellent agreement.

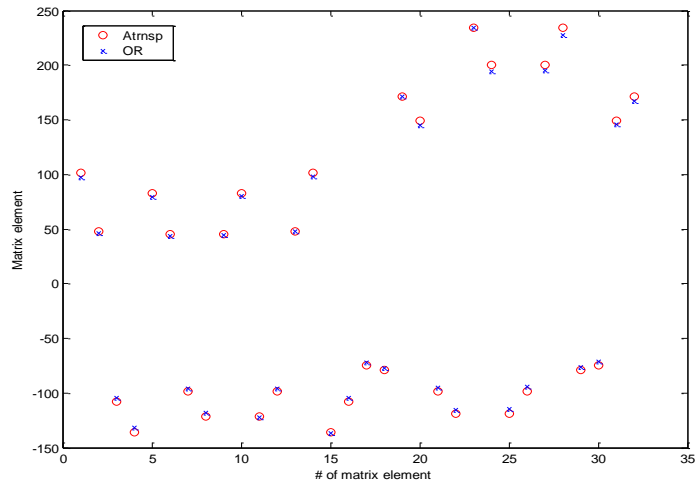


Fig. 11 Comparison of matrix from calculation and model matrix

## 5. Comparison

For comparing the measured matrix and the model matrix, the relative errors, defined here as  $(R_{ij_{meas}} - R_{ij_{model}})/R_{ij_{model}}$  are plotted in Fig. 12.

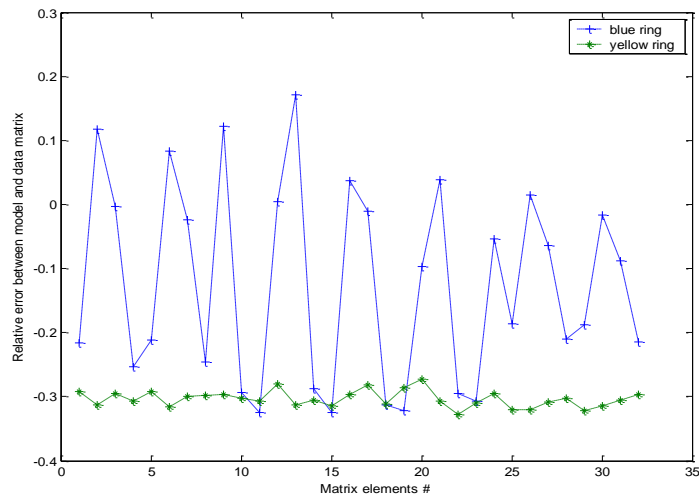


Fig. 12 Relative errors between measured matrix and model matrix

The relative error fluctuates roughly about  $\pm 10\%$  in the blue ring. However, the relative errors are always negative in the yellow ring, which could result if either BPM gain or corrector calibration is

incorrect. By assuming BPM gain or corrector calibration is 1.43 times smaller than design, one gets Fig. 13.

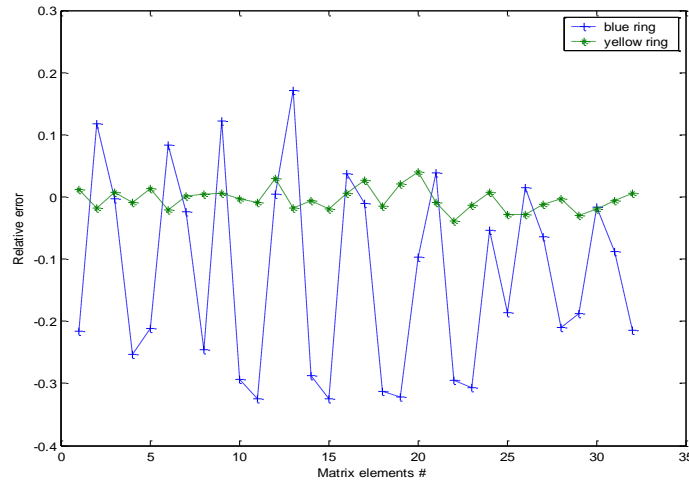


Fig. 13 Relative errors assuming BPM gain or corrector calibration offset

In addition to BPM gain and corrector calibration which both cause systematic errors, 10 Hz distortion introduces random error. Also, one needs to take into account the fact that the real matrix could be quite off the model matrix during store with small beta star at the two RHIC interaction points. One known source of systematic error concerns the difference between the designed tune and the measured tune. Fig. 14 shows the effect of a tune change on magnitude of a transfer matrix element in blue ring together with the design point and working point.

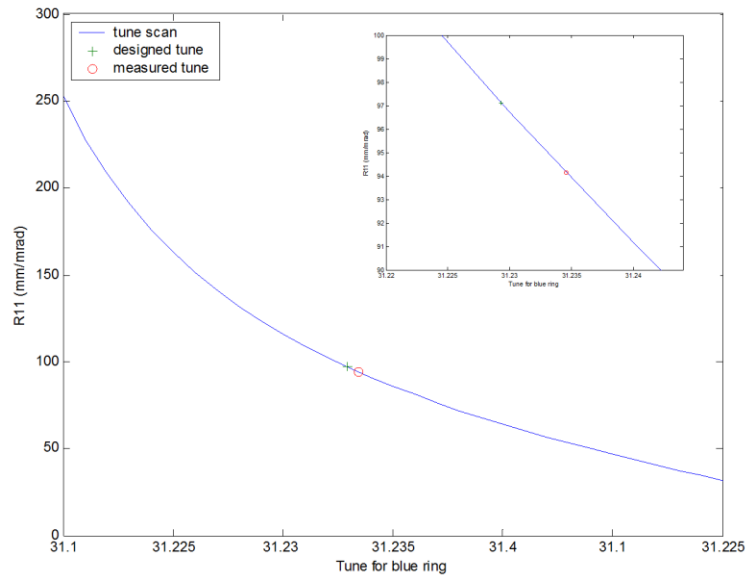


Fig. 14 Tune scan for one ORM element,  $R_{11}$

Fig. 15 shows the overall effect on relative errors by tune offset. Here, the design tune is 31.2293; the measured tune is 31.23455 from the beam transfer function acquired at approximately the same time as the ORM measurement.

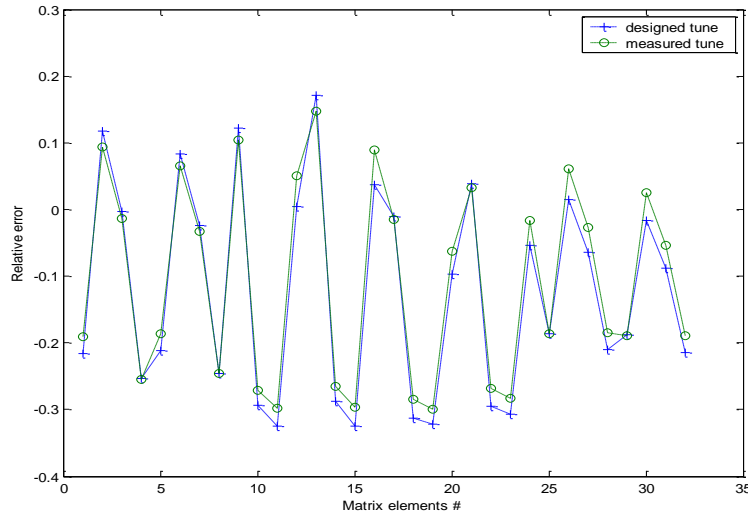


Fig. 15 Relative errors with designed tune and measured tune

With the measured tune, some of the big relative errors are reduced noticeably, however, increasing of errors of other individual matrix elements is also observed. As a speculation, amplitude detuning and change of beta functions during the measurements could be part of the reason for the discrepancy between measured and model matrix.

## 6. Clarified problems

The above results were reached after two problems, pertaining to the corrector ordering and the sign convention for correctors, were clarified. Initially the matrix of transfer functions elements had opposite sign compared to the model matrix in two of the four rows. The wrong corrector ordering was realized after checking the symmetry of the matrix. As shown in the schematic below, the elements are almost symmetrical to the axis, which result in very close numbers for certain matrix elements pairs.

Inspection of the model matrix revealed that it is composed of four sub matrices of the same symmetrical pattern which was not visible initially on the measured matrices. However, by rearranging the rows (which means changing the order of correctors), one obtained a matrix of the same symmetrical pattern. This led us to recheck the ordering and finally correct it.

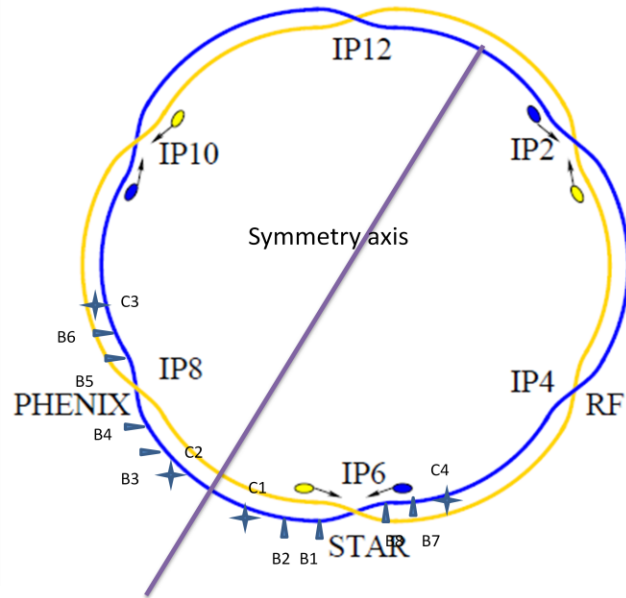


Fig. 16 Schematic of symmetrical elements arrangement

The signs of the measured and model matrix elements were then in agreement in the blue ring, however, the measured matrix elements for yellow ring has opposite signs with respect to the model. This turned out to be caused by a discrepancy in the sign convention of the 10 Hz gofb correctors compared to nominal RHIC convention. The dipole sign convention at RHIC is: positive deflection means positive BPM reading, also means outward or up deflection for both beams, which has the consequence that the orientation of the fields of the dipoles are opposite in the blue and yellow ring. However, the orientations for the 10 Hz feedback correctors were made during installation the same for both rings. It was reported that initial testing in the yellow ring diverged until sign flip implemented online.

## 7. Summary

Three methods for generating the response matrix from the measured data were presented. The results agree with each other reasonably well. Calculations of the orbit response matrix were given, which showed identical results and agreed with matrix from W. W. MacKay very well. After the wrong ordering of correctors and sign convention were clarified, the measured matrix and model matrix reached good agreement after including the systematic scaling factor correction in yellow, however, the discrepancy (30%) is not understood in blue.

As benefits to the future upgrade to the 10 Hz gofb system, algorithms were developed to process ORM data and generate measured transfer function elements and from these the measured SVD matrices; scripts were compiled (by A. Marusic) to extract Courant-Snyder parameters from the online OptiCalc model and generate model SVD matrices for fast turn-around of implementation when implementing a new optics.

## 8. Acknowledgements

The authors would like to thank K. Mernick, R. Michnoff, R. Hulsart, P. Thieberger, A. Marusic and W. W. MacKay for helpful discussions. We thank A. Marusic also for writing the script to extract Twiss parameters from OptiCalc.

## 9. References

- [1] C. Montag et al, Observation of helium flow induced beam orbit oscillations at RHIC, Nucl. Instr. & Meth. A 564 (2006) 26.
- [2] R. Bonati et al, Recent triplet vibration studies in RHIC, International Particle Accelerator Conference, 2010, Kyoto, Japan, p516-518.
- [3] M. Minty et al, <http://www.cadops.bnl.gov/Instrumentation/InstWiki/index.php/File:GlobalOrbitControlAlgorithm.pdf>.
- [4] K. Mernick, private communication.
- [5] S. Y. Lee (1993). *Accelerator Physics*. Singapore: World Scientific
- [6] H. Wiedemann (1995). *Particle Accelerator Physics II*. New York, NY: Springer.
- [7] W. W. MacKay, Calculating a closed orbit position and a response matrix, unpublished.

APPENDIX A: The Model ( $R_{\text{model}}$ ) and Measured Orbit Response Matrices (for blue ring) retrieved by three methods: by linear fitting ( $R_{\text{linearfit}}$ ), two frequencies curve fitting ( $R_{\text{curvefit}}$ ) and Fast Fourier Transforms ( $R_{\text{fft}}$ ).

```

R_model = 101.106880 82.813820 45.306130 48.098480 -74.280990 -98.304310 -119.084020 -79.206980
          48.098460 45.306130 82.814080 101.107180 -79.207300 -119.084450 -98.304380 -74.281050
          -107.633050 -98.574070 -121.601030 -135.593130 171.466210 233.961990 200.161650 148.803770
          -135.592600 -121.600580 -98.574140 -107.633160 148.803750 200.161650 233.961250 171.465680
R_linearfit = 76.142251 62.763918 49.959421 55.601407 -71.179376 -99.282189 -93.542909 -62.191289
             51.421914 46.987241 56.730301 69.850129 -53.090037 -81.710873 -95.594112 -70.006458
             -103.772317 -93.249530 -82.599584 -92.29597 116.20924 162.316078 182.755480 132.636283
             -98.316464 -89.020476 -96.379625 -108.764006 130.633162 184.210679 179.477255 131.053032
R_curvefit = 76.466568 63.090166 49.609571 54.866179 71.087273 98.406242 94.334368 62.504019
            51.470279 47.120033 57.085295 70.461960 53.268474 82.542409 95.716680 69.350031
            103.226225 92.739661 85.214287 95.220980 118.941662 166.141219 182.281208 132.766464
            97.103079 87.519830 97.059081 109.577372 131.107565 185.082404 177.534202 129.449579

```



R<sub>fit</sub> = 70.288767 57.954402 46.120612 51.330285 65.710083 91.659773 86.319917 57.380043  
50.881526 46.505956 56.105045 69.068914 52.500981 80.802931 94.542205 69.242810  
97.495329 87.615026 77.603981 86.722960 109.196179 152.488934 171.616956 124.560009  
96.368406 87.250870 94.451651 106.572041 128.013503 180.513698 175.902006 128.438486

## APPENDIX B: The Twiss Parameters at Correctors and BPMs for Blue Ring

Element/Parameters	s	betax	alphax	mux	mu
bo6-b1	25.0238	212.594	-8.34445	0.227572	31.2293
bo6-b3	36.8996	153.472	5.48348	0.234699	
bo7-b3	602.545	157.065	-5.61994	5.53388	
bo7-b1	614.421	217.706	8.5391	5.54084	
bi8-b1	664.469	214.332	-8.47189	6.00364	
bi8-b3	676.345	432.506	8.78525	6.01113	
bi5-b3	3796.95	423.977	-8.62612	30.9872	
bi5-b1	3808.82	210.409	8.30087	30.9949	
bo6-kfbh3	40.6386	121.378	4.72657	0.239173	
bo7-kfbh3	599.88	122.658	-5.06699	5.53089	
bi8-kfbh3	679.752	384.519	8.16926	6.01248	
bi5-kfbh3	3794.47	372.11	-8.18582	30.9863	

## APPENDIX C: The MatLab code for calculating ORM

```
% Calculating ORM based on Wiedeman
for i=1:4
    for j=1:8
        OR(i,j)=sqrt(data(i+8,2)*data(j,2))*cos(pi*data(1,5)-abs(2*pi*(data(i+8,4)-data(j,4))))/2/sin(pi*data(1,5));
    end
end

l=[1,0;0,1];
mu=2*pi*data(1,5);
for i=1:4
    for j=1:8
        M=[cos(mu)+data(j,3)*sin(mu) data(j,2)*sin(mu);
```

```

    -(1+data(j,3)^2)/data(j,2)*sin(mu),cos(mu)-data(j,3)*sin(mu)]; % one turn transfer matrix
if data(j,1)>data(i+8,1)
    phi=2*pi*(data(j,4)-data(i+8,4));
else
    phi=2*pi*(data(1,5)+data(j,4)-data(i+8,4));
end
M2=[sqrt(data(j,2)/data(i+8,2))*(cos(phi)+data(i+8,3)*sin(phi)),sqrt(data(j,2)*data(i+8,2))*sin(phi);
    -(1+data(i+8,3)*data(j,3))/sqrt(data(j,2)*data(i+8,2))*sin(phi)+(data(i+8,3)-
data(j,3))/sqrt(data(j,2)*data(i+8,2))*cos(phi),
    sqrt(data(i+8,2)/data(j,2))*(cos(phi)-data(j,3)*sin(phi))]; % transfer matrix from corrector to BPM
M3=inv(I-M)*M2; % closed-loop transfer matrix from corrector to BPM
% M1=inv(M2)*M;
% M3=(M2-inv(M1))/2/(1-cos(mu));
MWaldo(i,j)=M3(1,2); % based on Waldo

C1=cos(mu/2)/2/sin(mu/2)*data(i+8,2);
C2=(sin(mu/2)-data(i+8,3)*cos(mu/2))/2/sin(mu/2);
Msy(i,j)=M2(1,:)*[C1,C2]'; % based on S.Y. Lee
end
end

```

Remark: the Twiss parameter in Appendix B was imported to MatLab as a 12 by 5 matrix named *data*.